The Al-Au (Aluminum-Gold) System

26.98154 196.9665

By J.L. Murray*
National Bureau of Standards
and
H. Okamoto** and T.B. Massalski
Carnegie-Mellon University

Equilibrium Diagram

Nearly all of the important features of the Al-Au phase diagram (Fig. 1) were known at the end of the last century, primarily because of the work of [00Hey], which for the most part was accepted by [Hansen]. Further information published in [Shunk] did not alter the phase diagram of [Hansen] significantly. The present assessment of the Al-Au system updates the phase diagram according to the most recent experimental and theoretical work, primarily concerning the details of the thermodynamic evaluation of this system, but also involving information on the crystal structures of the various phases, metastable equilibria, and pressure effects.

The equilibrium phases in Fig. 1 are: (1) the fcc terminal solid solution (Al), having maximum solid solubility of 0.06 at.% Au at 650 °C; (2) the CaF_2-type intermediate phase Al_2Au, with homogeneity of 32.92 to 33.92 at.% Au; (3) the monoclinic intermediate phase AlAu with no appreciable solubility range; (4) the $MoSi_2$-type intermediate phase $\gamma AlAu_2$, with homogeneity of 65 to 66.8 at.% Au, and with two low-temperature allotropic forms of distorted $MoSi_2$-type structures, $\beta AlAu_2$ and $\alpha AlAu_2$; (5) the rhombohedral phase Al_2Au_5; (6) the bcc intermediate phase, β; (7) the distorted βMn-type $AlAu_4$, having the solubility range between 80 and 81.2 at.% Au; and (8) the fcc terminal solid solution (Au), with maximum solid solubility of 16 at.% Al at 545 °C. Special points of the equilibrium diagram (Fig. 1) are summarized in Table 1, where most of the listed invariant temperatures were determined by [00Hey]. Minor modifications in these temperatures may be necessary in the future because the melting points of Al and Au assumed by [00Hey] to be 655 and 1062.2 °C, respectively, are now accepted as 660.452 and 1064.43 °C [Melt].

Liquidus. The experimental liquidus data are shown in Fig. 2. The present thermodynamic calculations successfully represent the liquidus boundary (see "Thermodynamics").

*Present address: Alcoa Technical Center, Alloy Technology Division, Alcoa Center, PA 15069.
**Present address: ASM International, Metals Park, OH 44073.

Fig. 1 Assessed Al-Au Phase Diagram

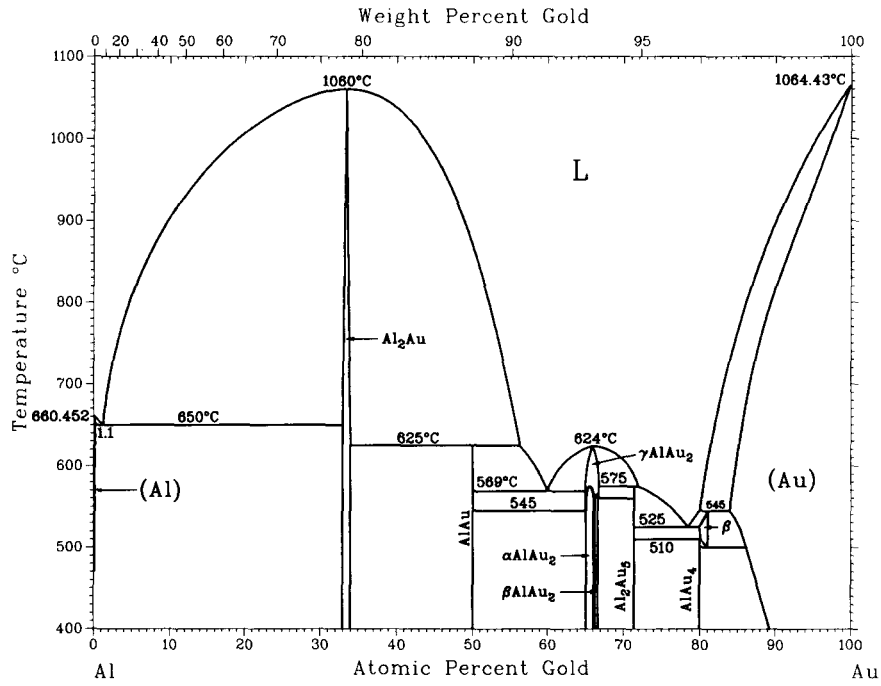

J.L. Murray, H. Okamoto, and T.B. Massalski, 1987.

Al Terminal Solid Solution, (Al). (Al) forms from the liquid by the eutectic reaction L ⇄ (Al) + Al_2Au. The eutectic point has been determined twice: as 0.7 at.% Au at 642 °C by [38Age] and as 1.1 at.% Au at 648 °C by [00Hey]. The latter value is relative to the 655 °C measured for the melting point of pure Al by [00Hey].

In a directional solidification study, [76Pia] found eutectic microstructures in the range between 1.1 and 1.7 at.% Au. In a faceted-nonfaceted eutectic system, the composition range in which eutectic microstructure is observed is skewed toward the faceted phase (Al_2Au). Assuming a theoretical model for predicting the coupled eutectic zone, [76Pia] found that the liquidus slope and the eutectic composition given by [00Hey] were more consistent with their experimental observations than the corresponding values given by [38Age].

The present thermodynamic calculations also support this view. According to these calculations, the (Al) liquidus slope is that predicted by the van't Hoff relation for the dilute limit, and the liquidus is a straight line over the relevant temperature range. The slope of the [00Hey] liquidus data agrees with the thermodynamic prediction, but the [38Age] value would require a significant deviation from the van't Hoff limit. The evaluators therefore

Table 1 Special Points of the Assessed Al-Au Phase Diagram

Reaction	Compositions of the respective phases, at.% Au			Temperature, °C	Reaction type
L ⇄ (Al) + Al_2Au	1.1	0.06	32.92	650	Eutectic
L + $AlAu_2$ ⇄ AlAu	56.5	33.92	50	625	Peritectic
L ⇄ AlAu + $\gamma AlAu_2$	60	50	65	569	Eutectic
$\gamma AlAu_2$ ⇄ AlAu + $\beta AlAu_2$	65	50	65.1	545	Eutectoid
$\gamma AlAu_2$ ⇄ $\alpha AlAu_2$ + $\beta AlAu_2$	66.2	66.3	66.1	560	Eutectoid
$\gamma AlAu_2$ ⇄ $\beta AlAu_2$ + $AlAu_5$	66.8	66.7	71.43	560	Eutectoid
L + $\gamma AlAu_2$ ⇄ Al_2Au_5	72.0	66.7	71.43	575	Peritectic
L ⇄ Al_2Au_5 + β	78.5	71.43	80	525	Eutectic
Al_2Au_5 + β ⇄ $AlAu_4$	71.43	80.2	80	510	Peritectoid
β ⇄ $AlAu_4$ + (Au)	81.1	80	86.2	~500	Eutectoid
L + (Au) ⇄ β	80	84	81.2	545	Peritectic
L ⇄ $\gamma AlAu_2$		66		624	Congruent point
$\gamma AlAu_2$ ⇄ $\alpha AlAu_2$		66.5		~565	Congruent point
$\gamma AlAu_2$ ⇄ $\beta AlAu_2$		65.6		~575	Congruent point
L ⇄ Al_2Au		33.3		1060	Congruent point
L ⇄ (Al)		0		660.45	Melting point
L ⇄ (Au)		100		1064.43	Melting point

Fig. 2 Experimental Data on the Liquidus and the (Au) Solidus and Solvus

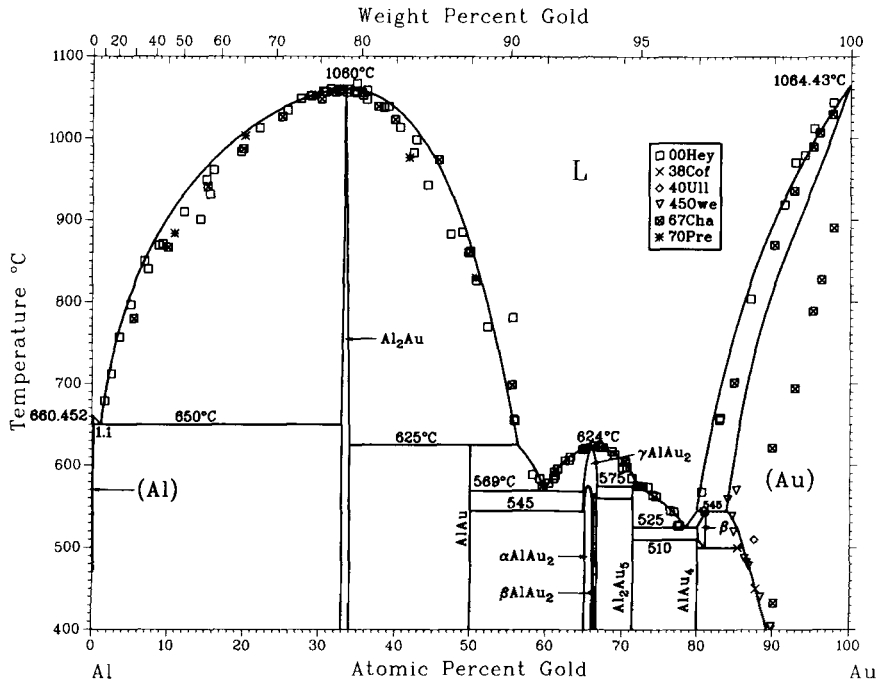

J.L. Murray, H. Okamoto, and T.B. Massalski, 1987.

Fig. 3 Al-Rich Part of the Diagram

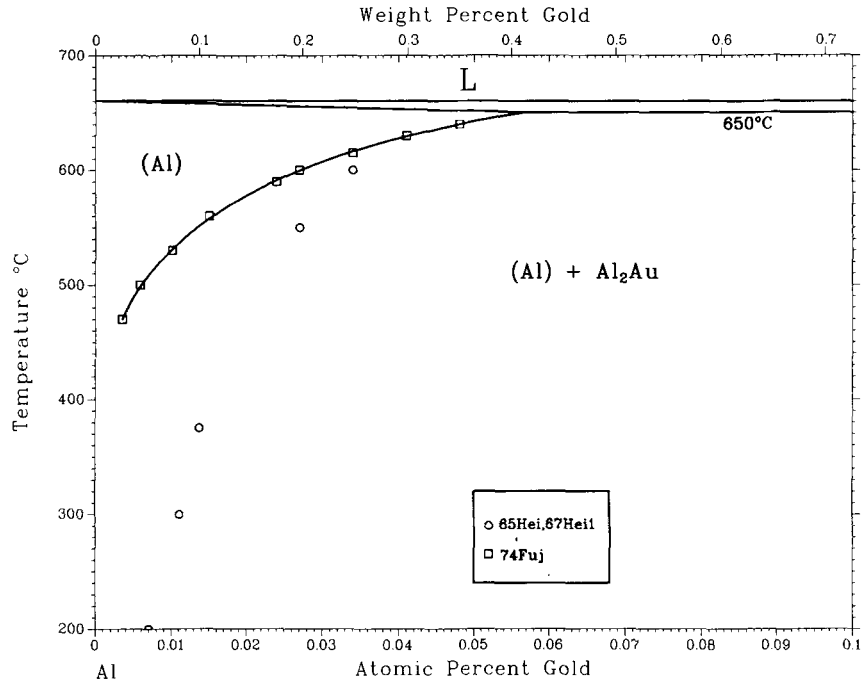

J.L. Murray, H. Okamoto, and T.B. Massalski, 1987.

Fig. 4 $AlAu_2$ Region of the Diagram

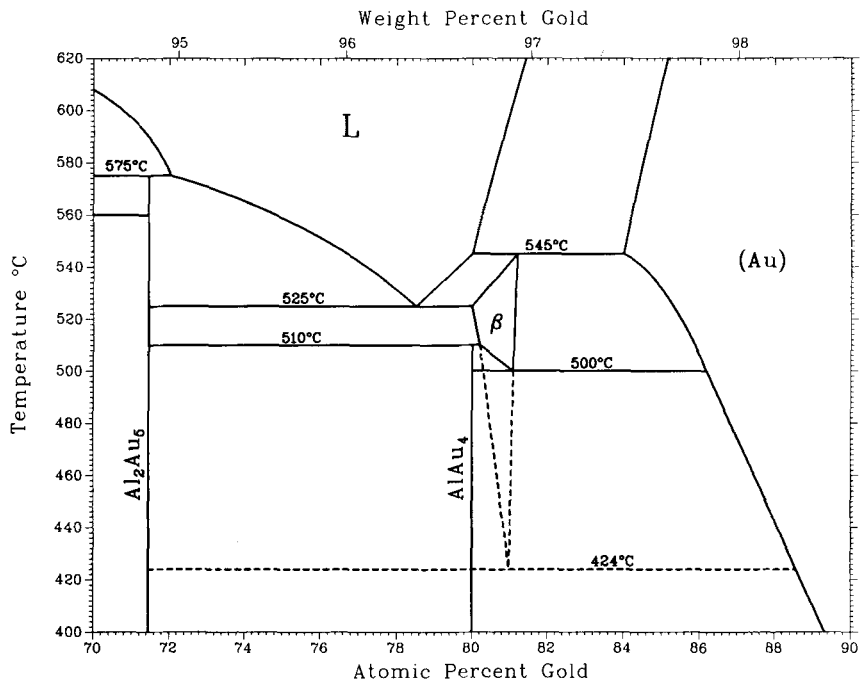

J.L. Murray, H. Okamoto, and T.B. Massalski, 1987.

place the eutectic point at 650 ± 3 °C and 1.1 ± 0.4 at.% Au.

The accepted solid solubility of Au in the (Al) terminal solid solution was obtained from the electrical resistivity measurements of [74Fuj]. The following solubility values were reported before [74Fuj] and may not represent the true equilibrium conditions: 0.03 to 0.06 at.% Au at 600 °C, based on microhardness measurements [65Hei, 67Hei1]; 0.08 to 0.1 at.% Au at 610 to 640 °C, estimated from the decrease in the lattice parameters [64Str2]; or less than 0.15 at.% Au at 642 °C, at which composition inclusions of the second phase were observed [38Age]. Solubility data are shown in Fig. 3.

Al_2Au. The existence of the purple-colored phase Al_2Au was firmly established by many investigators [1892Rob, 00Hey, 34Wes, 37Zin, 38Cof, 40Ull, 64Str1] by thermal, microscopic, and X-ray methods. According to the lattice parameter measurements of [64Str1], the homogeneity of Al_2Au could be bracketed between 32.92 and 33.92 at.% Au for alloys furnace cooled from temperatures between 400 and 300 °C.

AlAu. Although a completely single-phase alloy was not obtained, [00Hey] correctly predicted the existence of AlAu based on thermal and microscopic work. X-ray patterns indicated that the stability of AlAu is limited to a very narrow composition range [38Cof].

$AlAu_2$. [00Hey] reported the occurrence of $AlAu_2$, stable below 624 °C, and [38Cof] and [40Ull] confirmed its existence. From the shifting of the X-ray diffraction lines, [38Cof] estimated the homogeneity to be between 64.0 and 66.4 at.% Au at 500 °C and between 65.4 and 66.4 at.% Au at 400 °C. [68Fra] found two different types of distorted $MoSi_2$-type structures, one in a thin-film sample and the other in a bulk specimen. Figure 1 is based on the X-ray diffraction work of [74Pus], who reported a high-temperature phase, $\gamma AlAu_2$, and two low-temperature allotropic phases, $\beta AlAu_2$ and $\alpha AlAu_2$. $\alpha AlAu_2$ may be identical to the phase identified by [68Fra]. The homogeneities are estimated to be between 65 and 66.8 at.% Au for $\gamma AlAu_2$, 65.1 to 66.1 at.% Au for $\beta AlAu_2$, and 66.3 to 66.7 at.% Au for $\alpha AlAu_2$ [74Pus]. A detail of the region is shown in Fig. 4.

Al_2Au_5 (or Al_3Au_8). The existence of Al_2Au_5 was proposed by [00Hey] and [14Hey1, 14Hey2], with some suggestion that this phase may actually have the Al_3Au_8 atomic ratio. X-ray measurements of [38Cof] indicated a phase within a composition range between 72.3 and 73.0 at.% Au, closer to Al_3Au_8. [Hansen] decided, based on the thermal analysis data of [00Hey], that the Al_2Au_5 formula is more likely. X-ray studies of [68Fra] showed that the epitaxially formed rhombohedral Al_2Au_5 contained an intergrown metastable second phase with a simple cubic structure. Thus there is still some ambiguity regarding the exact composition and crystal structure of the proposed $AlAu_5$ phase.

β and $AlAu_4$. In Fig. 1, a disordered bcc phase β is shown forming on cooling through the peritectic reaction L + (Au) ⇄ β at 545 °C, and subsequently decomposing by the eutectoid reaction β ⇄ $AlAu_4$ + (Au), at approximately 500 °C.

Fig. 5 Au-Rich Part of the Diagram, Showing Metastable Equilibria Involving β

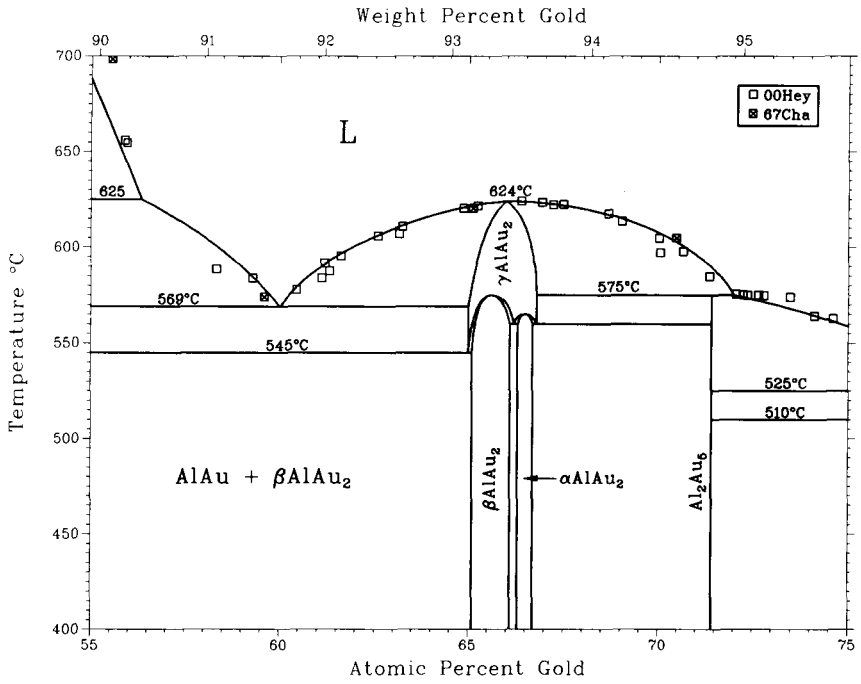

J.L. Murray, H. Okamoto, and T.B. Massalski, 1987.

The β phase was studied by [14Hey1] using thermal analysis and metallography, by [51Kuz] using X-ray diffraction, and by [68Fra] using electron microscopy. [14Hey1] found that the β phase could be undercooled to 424 °C, at which temperature the eutectoid reaction $\beta \rightleftarrows$ (Au) + Al_2Au_5 occurred with recalescence. An unknown phase "Y", which the current evaluators identify as $AlAu_4$, was formed by a reaction that consumed the Al_2Au_5. In forced recalescence experiments Al_2Au_5 was found to be metastable up to about 520 °C.

[51Kuz] and [68Fra] found that the disordered β phase transformed on cooling at about 400 °C to $AlAu_4$, and that the transformation on heating occurred at about 500 °C. The [Hansen] diagram, showing $\beta \rightleftarrows AlAu_4$ at about 400 °C, was constructed on the basis of the work of [51Kuz]. However, the evaluators note that the experimental observations of [51Kuz] and [68Fra] do not conflict with those of [14Hey1], and that, based on [14Hey1], the transition near 400 °C during cooling is a metastable one.

Figure 5 shows a detail of the Au-rich part of the diagram in which metastable extensions of the β phase boundaries are included. It is consistent with the results of [14Hey1, 51Kuz, 68Fra]. The boundaries of the β phase can be extrapolated to the metastable eutectic reaction at 424 °C. The compound $AlAu_4$, once formed, is stable to ~510 °C, at which temperature the equilibrium reaction $AlAu_4 \rightleftarrows Al_2Au_5 + \beta$ occurs.

Au Terminal Solid Solution (Au). The experimental boundaries of the (Au) phase with L + (Au), $\alpha AlAu_4$ + (Au), and $\beta AlAu_4$ + (Au) by [38Cof], [40Ull], [45Owe], [67Cha], and [72Pre] are shown in Fig. 2. All the data except those from [67Cha] along the [L + (Au)]/(Au) boundary are reasonably represented by the present thermodynamic analysis.

Other Phases. [50Hum] reported the existence of a 7 to 4 electron compound phase Al_3Au_5. No other experimental evidence exists to confirm this [00Hey, 38Cof, 40Ull, 66Coo].

A βMn-type compound $AlAu_3$ was proposed by [29Wes] and [35Fag] near 75 at.% Au. This compound is probably the $AlAu_4$ phase.

Thin Films. Studies done on Al-Au thin films have provided a useful means of finding the equilibrium phases and crystal structures, especially with regard to the phases AlAu and Al_2Au_5, which form very sluggishly by peritectic reactions. According to many investigations using various methods [31Eis, 62Wea, 65Ter, 70Aru, 70Wea, 71Abr, 72Kol, 74Cam, 75Cam, 79Maj, 80Gal, 81Maj, 81Mar, 81Van], almost all of the stable interme-

Fig. 6 Map of Phase Observed in Thin Films as a Function of Overall Composition and Annealing Temperature

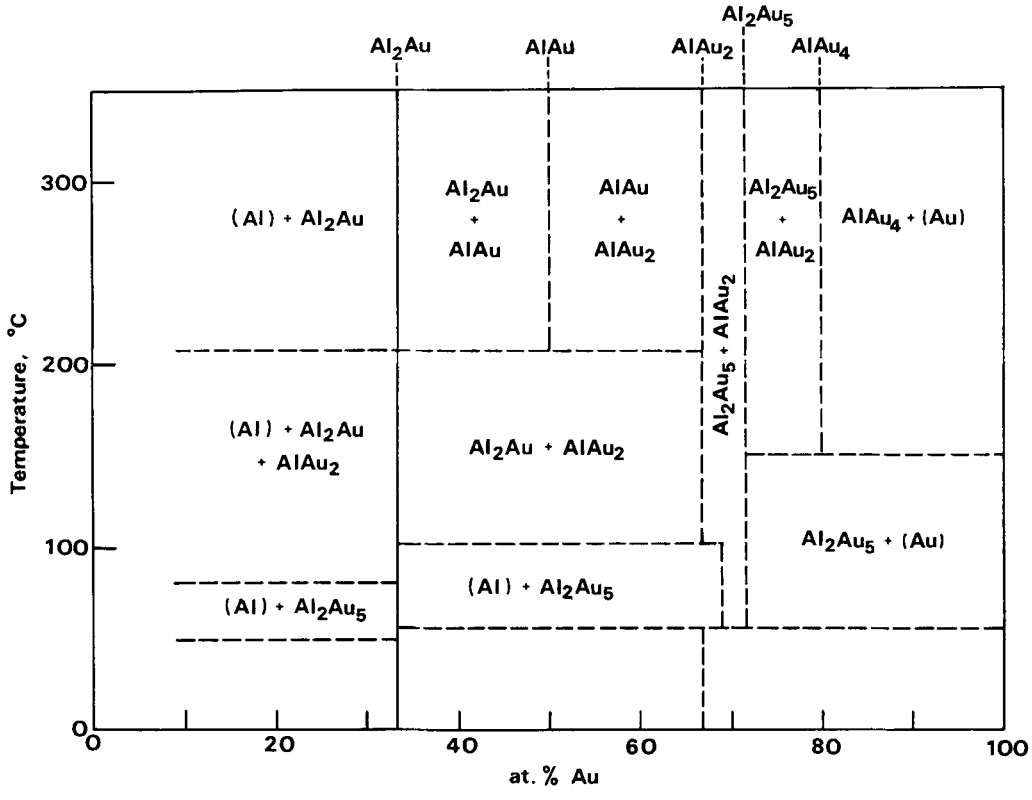

From [81Van].

J.L. Murray, H. Okamoto, and T.B. Massalski, 1987.

diate phases also form in thin films if appropriate conditions are fulfilled. The primary controlling factors are (a) the overall composition of the film, (b) the thickness, (c) the preparation method, (d) the annealing temperature, and (e) the strain energy contribution when the product phase forms from the component elements. Nevertheless, the phase that forms first seems to be either Al_2Au, Al_2Au_5, or $AlAu_2$. This is understandable because the Gibbs energies of formation of these three compounds are similar (see "Thermodynamics"). Secondary products also

Table 2 Al-Au Crystal Structure Data

Phase	Homogeneity, at.% Au	Pearson symbol	Space group	Strukturbericht designation	Prototype
(Al)	0 to 0.06	*cF*4	*Fm*3*m*	*A*1	Cu
Al_2Au	32.92 to 33.92	*cF*12	*Fm*3*m*	*C*1	CaF_2
AlAu	50	*mP*8	$P2_1/m$	*B*31	MnP
$\gamma AlAu_2$	65 to 66.8	*tI*6	*I*4/*mmm*	$C11_b$	$MoSi_2$
$\beta AlAu_2$	65.1 to 66.1	*oP*30	*Pnmn*	...	~$MoSi_2$
$\alpha AlAu_2$	66.3 to 66.7	*oP*12	*Pnma*	...	~$MoSi_2$
Al_2Au_5	71.43	(a)	...	...	...
β	80 to 81.2	*cI*2	*Im*3*m*	*A*2	W
$AlAu_4$	80	...	...	...	~βMn
(Au)	84 to 100	*cF*4	*Fm*3*m*	*A*1	Cu

(a) Rhombohedral.

Table 3 Al-Au Lattice Parameter Data

Phase	Composition, at.% Au	Lattice Parameters (a), nm *a*	*b*	*c*	Comments	Reference
(Al)	0	**0.42906**	...	...	25 °C	[King1]
Al_2Au	32.92	**0.599797**	...	...	25 °C	[64Str1]
	33.33	**0.599730**	...	...		
	33.92	**0.599695**	...	...		
	33.3	0.6000	...	...		[65Jan]
		0.5988	...	...	4.2 K	
	33	0.598	...	...	X-ray	[65Ter]
		0.6	...	...	ED(b)	
	33.33	**0.59973**	...	...	298 K	[72Str]
		0.59910	...	...	180	
		0.59891	...	...	140	
		0.59876	...	...	100	
		0.59871	...	...	80	
		0.59867	...	...	60	
		0.59864	...	...	40	
AlAu	50	0.6405	0.3333	0.6327	β = 92.99	[68Fra]
		0.6415	**0.3331**	**0.6339**	**β = 93.04**	[70Fra]
		0.3140	...	...	CsCl type	[71Abr]
$\gamma AlAu_2$	65 to 66.8	**0.3349**	...	**0.8893**		[74Pus]
$\beta AlAu_2$	65.1 to 66.1	**1.6772**	**0.3219**	**0.8801**		[74Pus]
$\alpha AlAu_2$	66.7	0.336	0.884	0.321	ED(b)	[68Fra]
		0.6755	**0.8871**	**0.3236**	X-ray	
	66.3 to 66.7	0.6715	0.8815	0.3219		[74Pus]
Al_2Au_5	71.43	**1.468**	...	...	**α = 30.5**	[68Fra]
		0.7719	...	4.196	(c)	...
		0.875	...	4.230	Hexagonal	[81Van]
β	80 to 80.2	**0.3236**	...	...		[51Kuz]
$AlAu_4$	80	0.6916	...	...		[40Ull]
	80	**0.69208**	...	...		[51Kuz]
(Au)	86.9	**0.40600**	...	...	(d)	[38Cof]
	89.9	**0.40644**	...	...		
	93.1	**0.40692**	...	...		
	96.4	**0.40737**	...	...		
	85.98	**0.40589**	...	...		[45Owe]
	88.44	**0.40624**	...	...		
	90.89	**0.40660**	...	...		
	93.22	**0.40697**	...	...		
	95.43	**0.40724**	...	...		
	98.26	**0.40762**	...	...		
	100	0.40781	...	...		
	100	**0.40784**	...	...	25 °C	[King1]

Note: The assessed values are in boldface type.
(a) Measured at room temperature unless otherwise specified. (b) Electron diffraction. (c) Equivalent hexagonal. (d) From graph.

form as a result of interdiffusion between the primary products and the pure elements. The secondary phase may further interdiffuse with the pure elements as long as the supply of constituent components lasts, and until stable or metastable equilibrium is reached. The end products are largely dependent on the overall composition. However, if the temperature is too low, or the thickness of the products becomes excessive, the intermediate products will tend to remain as metastable phases. A diagram was given by [81Van] (Fig. 6), which shows the interdependence between the overall composition and the observed phases in relation to the annealing temperature. The samples were heated slowly from 35 to 350 °C at a rate of 0.38 °C/min, where the thickness of one component was kept constant (Al = 200 nm for <33 at.% Au, Au = 200 nm for >33 at.% Au alloys). The overall results of work with thin films suggest that in most instances the equilibrium condition established in thin films may be equally valid for bulk specimens (see the section on $AlAu_2$ for a possible exception).

Metastable Phases

Using rapid solidification, the maximum solubility of Au in (Al) can be increased from the equilibrium value of 0.06 to 0.35 at.% Au [69Tod].

A large age-hardening effect is found in Al-rich alloys [65Hei, 67Hei2, 76Hei1, 76Hei2, 76San1, 76San2, 79Kon]. [67Hei2, 76Hei1, 76Hei2] reported that a metastable tetragonal phase η', distinct in structure from Al_2Au, precipitates in the form of coherent platelets during the early stages of aging. [76San1, 76San2], on the other hand, reported that the precipitates consist of the equilibrium phase, which is distorted by the constraint of coherency with the matrix. [76San1, 76San2] proposed a mechanism for the loss of coherency of the precipitates. [79Kon] verified the mechanism of continuous lattice accommodation and suggested that additional diffraction lines previously attributed to η' may be explained by double diffraction.

Crystal Structures

Crystal structure data for the stable phases in the Al-Au system are listed in Table 2. The experimentally determined lattice parameters are given in Table 3.

Al_2Au. The CaF_2-type structure was first established by [34Wes].

AlAu. X-ray and electron diffraction patterns of vapor-deposited thin films and powder specimens were indexed by [68Fra] as corresponding to a monoclinic structure. The structure derived by [70Fra] (see Table 2) from an X-ray diffraction pattern is very similar to that of [68Fra]. [68Fra] reported that determination of the AlAu structure from an electron diffraction pattern alone can lead to erroneous orthorhombic structure with two of the unit cell dimensions being nearly equal. The ZnS-type structure attributed to AlAu by [31Eis] and CsCl-type structure identified by [71Abr] from an electron diffraction pattern in thin films may be because of the same difficulty as that encountered by [68Fra].

$AlAu_2$. The high-temperature allotropic form $\gamma AlAu_2$ has the $MoSi_2$-type tetragonal structure [74Pus]. $\alpha AlAu_2$ has a distorted orthorhombic structure [68Fra, 74Pus]. $\beta AlAu_2$ is also orthorhombic, but with a larger unit cell [74Pus] (see Table 2).

Al_2Au_5. The rhombohedral structure of Al_2Au_5 was deduced from the X-ray and electron diffraction studies of [68Fra]. The complex electron diffraction pattern found in an epitaxially grown thin film is due to the coexistence of Al_2Au_5 and an intergrown second phase with an unknown simple structure (a = 0.64 nm). The report by [38Cof] that Al_2Au_5 has a complex structure similar to γbrass, but with a hexagonal distortion, is considered incorrect.

β Phase. The W-type bcc structure of β established by [51Kuz] was confirmed by [68Fra].

$\alpha AlAu_4$. The structure of $\alpha AlAu_4$ was considered to be βMn type [29Wes, 31Kat1, 31Kat2, 35Fag, 38Cof]. However, [40Ull] and [51Kuz] found that the structure is not exactly βMn type, but is slightly distorted.

Thermodynamics

Experimental Data. Experimental data for this system are available for the enthalpies of formation of the solid phases [66Fer, 72Pre], the enthalpy of mixing for the liquid [71Ita], and partial Gibbs energies in the liquid phase [67Cha, 69Lee, 70Pre, 70Yaz, 79Erd]. Experimental data for the enthalpies of formation and mixing are given in Table 4.

Measurements from which activities of partial Gibbs energies for the liquid phase can be derived were made by the following experimental techniques:

Thermodynamic quantity	Technique	Reference
G_{Al}	emf, 660 to 1100 °C	[67Cha]
	emf, 660 to 1150 °C	[70Pre]
	emf, 700 to 980 °C	[69Lee, 70Yaz]
G_{Au}	distribution method (Al-Au-Pb)	
G^{ex}_{Al}, G^{ex}_{Au}	Knudsen cell, mass spectrometry, 1267 to 1387 °C	[79Erd]

Partial Gibbs energies G_{Au} were derived by [67Cha], [69Lee], [70Pre], and [70Yaz] using Gibbs-Duhem integration. There are major discrepancies among these results, as illustrated by Fig. 3, taken from [79Erd].

Similar conflicts exist in the derived excess entropies for the liquid phase, $S^{ex}(L)$. [67Cha] obtained a nearly ideal entropy of mixing, [70Pre] a positive entropy of mixing (with maximum ~8 J/mol·K) and [69Lee, 70Yaz, 79Erd] a negative entropy of mixing (minimum approximately −10 J/mol·K [79Erd]; approximately −7 J/mol·K, [69Lee, 70Yaz]).

The present optimization calculations verify the negative $S^{ex}(L)$ but do not support the behavior of $G^{ex}(L)$ as proposed by [79Erd]. However, because many discrepancies or inaccuracies of the phase diagram are not yet resolved, the present calculations are far from conclusive. Further

Table 4 Al-Au Experimental Thermodynamic Data

Phase	Composition, at.% Au	Temperature, °C	Enthalpy of formation, $\Delta_f H$(s), J/mol	Enthalpy of mixing, $\Delta_{mix} H$(L), J/mol	Reference
Al_2Au	33.5 ± 0.5	127	−41 422		[66Fer]
	33.3	500	−39 162		[70Pre]
AlAu	50	500	−32 551		[70Pre]
	49.7 ± 0.3	127	−36 400		[66Fer]
$AlAu_2$	66.7 ± 0.3	127	−35 355		[66Fer]
	66.7	500	−27 614		[70Pre]
(Au)	83.0 ± 1.5	127	−22 594		[66Fer]
	95	500	−4 393		[70Pre]
	90	500	−8 033		
	88	500	−9 623		
L	10	1100		−5 854	[71Ita]
	20			−10 952	
	30			−15 013	
	40			−17 794	
	50			−19 186	
	60			−20 209	
	70			−18 676	
	80			−14 796	
	90			−8 473	

experimental work on the phase diagram and further calculations are needed.

Calculation of the Phase Diagrams. The present optimization calculations make use of the assessed phase diagram data, $\Delta_f H$ of the solid phases, $\Delta_{mix} H$ of the liquid [71Ita], and partial Gibbs energies of the liquid [79Erd].

The intermetallic phases were represented as line compounds, for which the Gibbs energy of phase i is:

$$G^0(i) = H^0(i) - TS^0(i)$$

Because of the lack of definitive phase diagram data in the β region, no distinction is made between the disordered bcc phase β and the intermetallic compound $AlAu_4$. They are modeled as a single line compound $AlAu_4$. Similarly, the three forms—$\gamma AlAu_2$, $\beta AlAu_2$, and $\alpha AlAu_2$—are not distinguished for the purpose of the calculations.

The excess Gibbs energies of the fcc and liquid solution phases are represented as:

$$G^{ex}(i) = \Sigma_j B_j(i,T)\, x(1\text{-}x)\, P_j\, (1-2x)$$

where i is the phase; x, the atom fraction Au; B_j, the coefficient of the j^{th} Legendre polynomial in the expansion; and T, the temperature in K.

A temperature-dependent subregular solution model has been chosen for G^{ex}. This choice is based on a series of calculations using different numbers of terms in the expansion. For higher than subregular solutions, the scatter in the Al_2Au liquidus data [00Hey] is (artificially) reproduced by the calculations.

Thermodynamic parameters from the present calculations are listed in Table 5 and the calculated diagram is shown in Fig. 7. The Al_2Au and (Au) liquidus branches are reproduced by the present calculation within the experimental uncertainty. The calculated Al_2Au_5 liquidus lies somewhat above the experimental data, consistent with the observation of undercooling in this system. The calculated (Au) solidus is consistent with the rough estimate of [00Hey] and not with the emf data of [67Cha]. As mentioned above, qualitative agreement was obtained with enthalpies of mixing for the liquid [71Ita], but not with the most recent and comprehensive activity data [79Erd].

Table 5 Al-Au Thermodynamic Parameters

Properties of the Pure Components

$G^0(Al, L) = 0$
$G^0(Au, L) = 0$
$G^0(Al, fcc) = -10\,780 + 11.548\,T$
$G^0(Au, fcc) = -12\,552 + 9.393\,T$

Excess Functions

$B_0(L) = -105\,252 + 41.299\,T$
$B_1(L) = 34\,184$
$B_0(fcc) = -53\,513 + 3.546\,T$
$B_1(fcc) = -272 + 30.995\,T$
$B_2(fcc) = 17\,305$

Compounds

$G^0(Al_2Au) = -33\,750 + 13.566\,T$
$G^0(AlAu) = -42\,564 + 22.388\,T$
$G^0(AlAu_2) = -37\,638 + 17.069\,T$
$G^0(Au_2Au_5) = -35\,078 + 15.772\,T$
$G^0(AlAu_4) = -23\,328 + 6.332\,T$

Values in J/mol, J/mol·K.

Pressure

The melting point of Al_2Au decreases with pressure at the rate of 5 °C/GPa at least up to 5 GPa [66Sto]. According to [66Sto], the negative derivative dT/dp suggests the existence of an allotropic phase transition at a still higher pressure.

Addendum

The Al-Au system, as contributed in a short version by R.P. Elliott and F.A. Shunk, was published in provisional form in the *Bulletin* [81Ell]. The present evaluation reviews all bibliography and data on the Al-Au system available in the literature through 1983 and includes in-

Fig. 7 Calculated Al-Au Phase Diagram

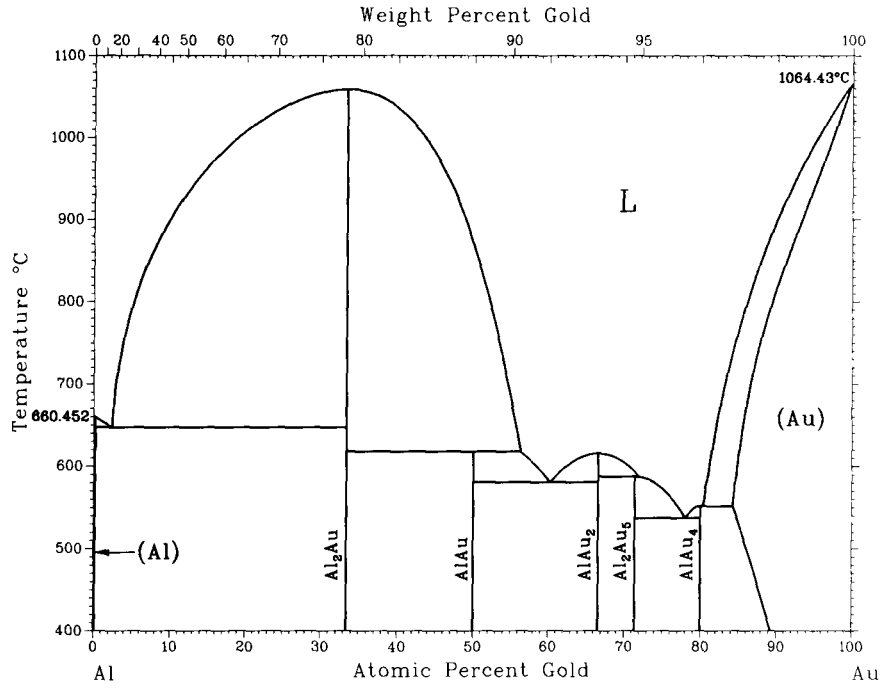

J.L. Murray, H. Okamoto, and T.B. Massalski, 1987.

formation pertaining to crystal structures, metastable phases, thermodynamics, and pressure. The present authors have also performed a thermodynamic assessment of certain phase boundaries. The present evaluation supersedes the earlier work.

Cited References

1892Rob: W.C. Roberts-Austen, "On the Melting Points of the Gold Aluminum Series of Alloys," *Proc. R. Soc. (London), 50*, 367-368 (1891-1892). (Equi Diagram; Experimental)

***00Hey:** C.T. Heycock and F.H. Neville, "Gold-Aluminium Alloys," *Philos. Trans. R. Soc. (London), 194*, 201-232 (1900). (Equi Diagram; Experimental; #)

14Hey1: C.T. Heycock and F.H. Neville, "Dilute Solutions of Aluminum in Gold," *Proc. R. Soc. (London), 214*, 267-276 (1914). (Equi Diagram; Experimental; #)

14Hey2: C.T. Heycock and F.H. Neville, "Dilute Solutions of Aluminum in Gold," *Proc. R. Soc. (London), 90*, 560-562 (1914). (Equi Diagram; Experimental; #)

29Wes: A. Westgren and G. Phragnem, "X-Ray Studies on Alloys," *Trans. Faraday Soc., 25*, 379-385 (1929). (Equi Diagram; Experimental; #)

31Eis: O. Eisenhut and E. Kaupp, "Investigation of Gold-Copper Alloys by the Refraction of Rapid Electrons," *Z. Elektrochem., 37*, 466-473 (1931). (Equi Diagram, Crys Structure; Experimental)

31Kat1: N. Katoh, "X-Ray Investigation of the Gold-Aluminum System. I," *J. Chem. Soc. Jpn., 52*, 851-854 (1931). (Crys Structure; Experimental)

31Kat2: N. Katoh, "X-Ray Investigation of the Gold-Aluminum System. II," *J. Chem. Soc. Jpn., 52*, 854-856 (1931). (Crys Structure; Experimental)

34Wes: C.D. West and A.W. Peterson, "The Crystal Structure of $AuAl_2$," *Z. Krist A, 88*, 93-94 (1934). (Equi Diagram, Crys Structure; Experimental)

35Fag: S. Fagerberg and A. Westgren, "The Crystal Structure of β-Manganese and Isomorphous Alloys," *Metallwirtschaft, 14*, 265-267 (1935) in German. (Equi Diagram, Crys Structure; Experimental)

37Zin: E. Zintl, A. Harder, and W. Haucke, "Metals and Alloys. XXII. Alloy Phases with Fluorite Structure," *Z. Physik. Chem., B, 35*, 354-362 (1937) in German. (Equi Diagram; Experimental)

38Age: N. Ageew and V. Ageewa, Discussion in [38Cof], *Trans. Metall. AIME, 128*, 258-260 (1938). (Equi Diagram; Experimental; #)

***38Cof:** A.S. Coffinberry and R. Hultgren, "The Gold-Aluminum System," *Trans. Metall. AIME, 128*, 249-258 (1938). (Equi Diagram, Crys Structure; Experimental; #)

***40Ull:** O.E. Ullner, "X-Ray Analysis of Gold-Aluminum Alloys," *Arkiv. Kemi. Mineral. Geol., 14A*(3), 1-20 (1940). (Equi Diagram, Crys Structure; Experimental; #)

45Owe: E.A. Owen and E.A.O. Roberts, "The Solubility of Certain Metals in Gold," *J. Inst. Met., 71*, 213-254 (1945). (Equi Diagram, Crys Structure; Experimental; #)

50Hum: W. Hume-Rothery, "*The Structure of Metals and Alloys*," Institute of Metals (London), 113 (1950). (Equi Diagram; Theory)

51Kuz: V.G. Kuznetsov and V.I Ravezova, "Structure of the Compound $AlAu_4$," *Dokl. Akad. Nauk., SSSR, 81*, 51-54 (1951) in Russian. (Equi Diagram, Crys Structure; Experimental)

62Wea: C. Weaver and L.C. Brown, "Diffusion in Evaporated Films of Gold-Aluminium," *Philos. Mag., 7*, 1-16 (1962). (Equi Diagram; Experimental)

64Str1: M.E. Straumanis and K.S. Chopra, "Lattice Parameters, Expansion Coefficients and Extent of the Al_2Au Phase," *Z. Physik. Chem. (Frankfurt), 42*(5-6), 344-350 (1964). (Equi Diagram, Crys Structure; Experimental)

64Str2: M.E. Straumanis, C.L. Woodard, and K.S. Chopra, "Influence of Small Amounts of Gold on the Lattice Parameter of Aluminum," *Z. Phys. Chem. (Frankfurt), 42*(1-2), 82-86 (1964). (Equi Diagram; Experimental)

65Jan: J.P. Jan, W.B. Pearson, Y. Saito, M. Springford, and I.M.

Templeton, "De Haas-van Alphen Effect and Fermi Surface of the Intermetallic Compounds $AuAl_2$, $AuGa_2$ and $AuIn_2$," *Philos. Mag, 12*(120), 1271-1291 (1965). (Crys Structure; Experimental)

65Hei: M.V. Heimendahl, "Tempering and Precipitation in the System Aluminum-Gold," *Phys. Status Solidi, 10*, K131-K133 (1965) in German. (Meta Phases; Experimental)

65Ter: L. Tertian and D. Darmagna, "Electron Diffraction Study of Gold-Aluminum Alloys," *Mem. Sci. Rev. Met., 62*(3), 207-214 (1965) in French. (Equi Diagram, Crys Structure; Experimental)

66Coo: C.J. Cooke and W. Hume-Rothery, "On the Structure of Copper, Silver, and Gold," *J. Less-Common Met., 10,* 52-56 (1966). (Equi Diagram; Experimental)

66Fer: R. Ferro, R. Capelli, and R. Marazza, "Alloys of Noble Metals with Highly Electropositive Elements. X. Heat of Formation of Aluminum-Gold Alloys, *Atti Accad. Naz. Lincie, Cl. Sci. Fis., Mat. Nat., Rend., 41*(1-2), 85-89 (1966) in Italian. (Thermo; Experimental)

66Sto: A.R. Storm, J.H. Wernick, and A. Jayaraman, "Fusion Behavior and Phase Changes at High Pressures in Some Intermetallic Compounds with Fluorite Structure," *J. Phys. Chem. Solids, 27*, 1227-1232 (1966). (Pressure; Experimental)

67Cha: D. Charquet, P. Desre, and E. Bonnier, "Determination of the Thermodynamic Properties and the Equilibrium Phase Diagram of the Au-Al System," *Compt. Rend., 264*(20), 1637-1640 (1967) in French. (Equi Diagram, Thermo; Experimental; #)

67Hei1: M. von Heimendahl, "The Solubility of Gold in Aluminum and the Precipitation Hardening of Aluminum-Gold Alloys," *Z. Metallkd., 58*(4), 230-235 (1967). (Equi Diagram, Meta Phases; Experimental)

67Hei2: M. von Heimendahl, "Precipitation in Aluminum-Gold," *Acta Metall., 15*(9), 1441-1452 (1967). (Meta Phases; Experimental)

***68Fra:** M.H. Francombe, A.J. Noreika, and W.J. Takei, "Thin Film and Bulk Structures of Phases in the System Gold-Aluminum," *Thin Solid Films, 1*(5), 353-366 (1968). (Equi Diagram, Crys Structure; Experimental)

69Lee: Y.K. Lee and A. Yazawa, "Thermodynamic Study of the Liquid Aluminum-Gold System," *Tohoku Daigaku Senko Seiren Kenkyusho Iho, 25*(1), 1-8 (1969) in Japanese. (Thermo; Experimental)

69Tod: T. Toda and R. Maddin, "The Mechanical Properties of Splat-Cooled Aluminum-Base Gold Alloys," *Trans. Metall. AIME, 245*(5), 1045-1054 (1969). (Meta Phases; Experimental)

70Aru: Arunsingh, O.N. Srivastava, and B. Dayal, "Production of Thin Alloy Single Crystals," *Z. Metallkd., 61*(5), 383-386 (1970). (Equi Diagram; Experimental)

70Fra: K. Frank and K. Schubert, "Crystal Structure of AuAl," *J. Less-Common Met., 22*(3), 349-354 (1970) in German. (Crys Structure; Experimental)

70Pre: B. Predel and U. Schallner, "Thermodynamic Investigation of the Aluminum-Antimony and Aluminum-Gold Systems," *Mater. Sci. Eng., 5*(4), 210-219 (1970) in German. (Equi Diagram, Thermo; Experimental; #)

70Wea: C. Weaver and D.T. Parkinson, "Diffusion in Gold-Aluminum," *Philos. Mag., 22*(176), 377-389 (1970). (Equi Diagram; Experimental)

70Yaz: A. Yazawa and Y.K. Lee, "Thermodynamic Studies of the Liquid Aluminum Alloy Systems," *Trans. Jpn. Inst. Met., 11*(6), 411-418 (1970). (Thermo; Experimental)

71Abr: G.K. Abramyan, A.N. Pilyankevich, and I.N. Frantsevich, "Structure of the Compound AuAl in the Form of a Thin Film," *Dokl. Akad. Nauk SSSR, 196*(5), 1054-1055 (Tech. Phys.) (1971) in Russian; TR: *Sov. Phys. Dokl., 16*(2), 138- 139 (1971). (Equi Diagram, Crys Structure; Experimental)

71Ita: K. Itagaki and A. Yazawa, "Measurements of Heats of Mixing in Liquid Gold Binary Alloys," *J. Jpn. Inst. Met., 35*(4), 389-394 (1971) in Japanese. (Thermo; Experimental)

72Kol: D.P. Kolesnikov, A.F. Andrushko, and Ye.I Sukhinina, "Interaction of Aluminum with Gold in Thin Films," *Fiz. Met. Metalloved, 34*(3), 529-534 (1972) in Russian; TR: *Phys. Met. Metallogr., 34*(3), 76-81. (Equi Diagram; Experimental)

72Pre: B. Predel and H. Ruge, "Thermodynamic Investigation of Solid Aluminum-Gold Alloys," *Z. Metallkd., 63*(2), 59-63 (1972) in German. (Thermo; Experimental)

72Str: M.E. Straumanis and J.S. Shah, "Low Temperature Lattice Parameters and Expansion Coefficients of Al_2Au and LiF — Gruneisen Constants of LiF," *Z. Anorg. Chem., 391*(1), 79-85 (1972). (Crys Structure; Experimental)

74Cam: S.U. Campisano, G. Foti, F. Grasso, J.M. Mayer, and E.Rimini, "Analysis of Compound Formation in Gold-Aluminum Thin Films," *Appl. Ion Beams Met.,* (Int. Conf.), 159-168 (1974). (Equi Diagram; Experimental)

***74Fuj:** S. Fujikawa and K. Hirano, "Solid Solubility of Gold in Aluminum," *J. Jpn. Inst. Met., 38*(10), 929-936 (1974) in Japanese. (Equi Diagram; Experimental)

***74Pus:** M. Puselj and K. Schubert, "Crystal Structure of the Au_2Al (h), Au_2Al_{1-} (r) and Au_2Al_{1-} (r) Phases," *J. Less-Common Met., 35*(2), 259-266 (1974). (Equi Diagram, Crys Structure; Experimental)

75Cam: S.U. Campisano, G. Foti, E. Rimini, S.S. Lau, and J.W. Mayer, "Kinetics of Phase Formation in Au-Al Thin Films," *Philos. Mag., 31*(4), 903-917 (1975). (Equi Diagram; Experimental)

76Hei1: M. von Heimendahl, "Structure of the Metastable η'-phase in Aluminum-Gold Alloys," *Z. Metallkd., 67*(3), 195-197 (1976) in German. (Meta Phases; Experimental)

76Hei2: M. von Heimendahl, "Comment on: 'Precipitation in Al-0.212 wt.% Au Alloy' by R. Sankaran and C. Laird," *Acta. Metall., Scr. Metall., 10*, 505 (1976). (Meta Phases; Experimental)

76Pia: G. Piatti and G. Pellegrini, "The Structure of the Unidirectionally Solidified Al-Al_2Au Eutectic," *J. Mater. Sci., 11*(5), 913-924 (1976). (Equi Diagram; Experimental)

76San1: R. Sankaran and C. Laird, "Precipitation in an Al-0.212 wt.% Au Alloy," *Acta Metall., 24*, 517-522 (1976). (Meta Phases; Experimental)

76San2: R. Sankaran and C. Laird, "Reply to Comments on Precipitation in Al-0.212 wt.% Au Alloy," *Scr. Metall., 10*(6), 507-508 (1976). (Meta Phases; Experimental)

79Erd: L. Erdelyi, J. Tomiska, A. Neckel, G. Rose, E.S. Ramakrishnan, and D.J. Fabian, "Thermodynamic Parameters of Liquid Gold-Aluminum Alloys," *Metall. Trans. A, 10*(10), 1437-1443 (1979). (Thermo; Experimental)

79Kon: H. Konig and M. von Heimendahl, "Precipitation Mechanism and Creep Behavior of an Al-0.2 wt.% Alloy," *Z. Metallkd., 70*(7), 419-425 (1979). (Meta Phases; Experimental)

79Maj: G. Majni, G. Ottaviani, and E. Galli, "AuAl Compound Formation by Thin Film Interactions," *J. Cryst. Growth, 47*(4), 583-588 (1979). (Equi Diagram; Experimental)

80Gal: E. Galli, G. Majni, C. Nobili, and G. Ottaviani, "Gold-Aluminum Intermetallic Compound Formation," *Proc. Electrocomponent Sci. Technol., 6*(3-4), 147-150 (1980). (Equi Diagram; Experimental)

***81Ell:** R.P. Elliott and F.S. Shunk, "The Al-Au (Aluminum-Gold) System," *Bull. Alloy Phase Diagrams, 2*(1), 70-75 (1981). (Equi Diagram; Compilation; #)

81Maj: G. Majni, C. Nobili, G. Ottaviani, M. Costato, and E. Galli, "Gold-Aluminum Thin-Film Interactions and Compound Formation," *J. Appl. Phys., 52*(6), 4047-4054 (1981). (Equi Diagram; Experimental)

81Mar: Z. Marinkovic and V. Simic, "Room Temperature Interactions in Au/Metal and Al/Metal Thin Film Couples," *Thin Solid Films, 75*(3), 229-235 (1981). (Equi Diagram; Experimental)

***81Van:** J.M. Vandenberg and R.A. Hamm, "A Continuous X-Ray Study of the Interfacial Reaction in Au-Al Thin Film Couples," *J. Vac. Sci. Technol., 19*(1), 84-88 (1981). (Equi Diagram, Crys Structure; Experimental)

* Indicates key paper.
\# Indicates presence of a phase diagram.

Al-Au evaluation contributed by **J.L. Murray,** Center for Materials Research, National Bureau of Standards, Gaithersburg, MD 20899, and **H. Okamoto** and **T.B. Massalski,** Department of Metallurgical Engineering and Materials Science, Carnegie-Mellon University, Pittsburgh, PA 15213. This work was supported by the Defense Advanced Research Project Agency (DARPA), the National Bureau of Standards through the Metallurgy Division and through the Office of Standard Reference Data, the International Gold Corporation, and ASM International. Literature searched through 1983. Dr. Murray is the ASM/NBS Data Program Category Editor for binary aluminum alloys. Professor Massalski is the ASM/NBS Data Program Editor-in-Chief for the binary alloys, and also Category Editor for binary gold alloys, jointly with Dr. Okamoto.

The H-Ti (Hydrogen-Titanium) System

1.00794 47.88

By A. San-Martin and F.D. Manchester
University of Toronto

Equilibrium Diagram

The assessed Ti-H phase diagram is shown in Fig. 1 and 2, which are sections of a P-T-X surface in the T-X plane and the P-X plane, respectively, where P is pressure in Pa, T is temperature in K and °C, and X is the hydrogen concentration, expressed as X = H/Ti (the atomic ratio). Two presentations are necessary for a hydrogen–metal system, because the equilibrium pressure of the hydrogen surrounding the metal is always a significant thermodynamic variable, in contrast to most situations involving metallic alloys. The participation of hydrogen in the various phases of alloy systems is the best available example of hydrogen acting as a metal [71Gil]. The crystal structures and lattice parameters of the Ti-H phases are given in Tables 1 and 2, respectively. Figure 3 illustrates the existing phase relationships at high pressure (50 MPa) reported by [83Sha].

Recent work [84Num, 85Woo] evaluating evidence on the existence of a metastable hydride phase in the Ti-H system led both [84Num] and [85Woo] to propose relabeling the phases in the Ti-H system to correspond with the designations for the isostructural Zr-H system.

The composite phase diagram (Fig. 1) is of the eutectoid type, and consists of the following phases: (1) cph α; (2) bcc β; 3) two interstitial solid solutions of hydrogen based on the allotropic α and β forms of pure Ti; (4) δ, a fcc hydride; (5) ε, a tetragonally distorted fcc or fct hydride with axial ratio $c/a < 1$; and (6) γ, a metastable fct hy-

Fig. 1 Assessed Ti-H Phase Diagram

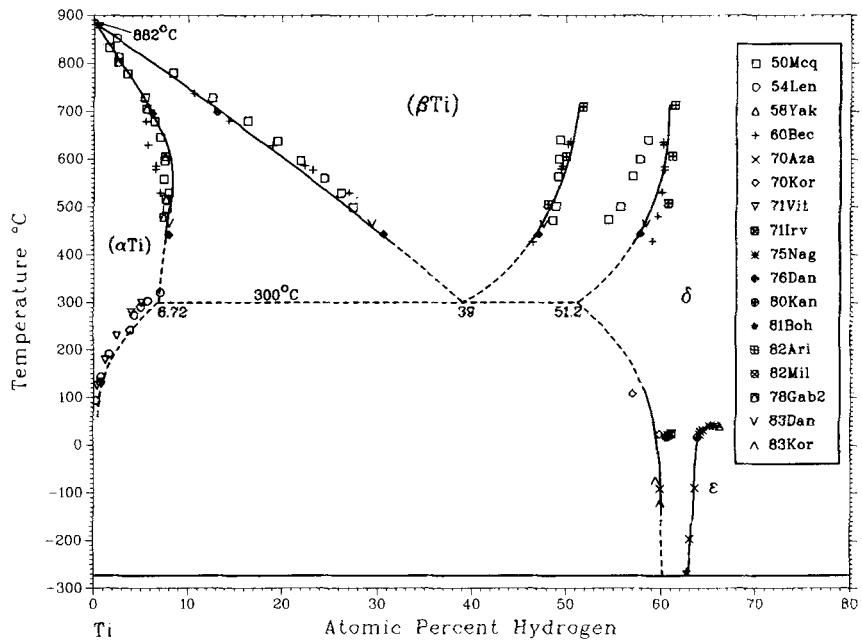

Projected on the T-X plane from a P-X-T surface. A. San-Martin and F.D. Manchester, 1987.